

Equilibrium geometry and electronic structure of the low-temperature W(001) surface

Rici Yu and H. Krakauer

Department of Physics, College of William and Mary, Williamsburg, Virginia 23187-8795

D. Singh

Complex Systems Theory Branch, Naval Research Laboratory, Washington, D.C. 20375-5000

(Received 29 July 1991)

The multilayer reconstruction of the W(001) surface at low temperature and the multilayer relaxation of the unreconstructed surface are investigated using first-principles total-energy and force calculations. The fully relaxed ideal surface is determined to be unstable by 110 meV per surface atom, which agrees qualitatively with results of previous studies where multilayer relaxation and reconstruction were not taken into account and supports the conclusion that the high-temperature phase is disordered. The lateral displacement of the second-layer atoms is about 18% that of the first-layer atoms and the first interlayer distance is contracted by about 6% from the bulk value in the reconstructed surface. The lateral displacements compare well with a recent x-ray-diffraction experiment. The electronic structure and the surface-state dispersions for the equilibrium reconstructed geometry are examined in detail.

A great many experimental and theoretical studies have been devoted to the understanding of the structure and phase transitions of the W(001) surface. Despite this fact, there are still unresolved problems regarding the structure and the nature of its high-temperature phase. By contrast, the structure of the low-temperature phase, as described by the Debe-King (DK) model,¹ appears to be well established. Nevertheless, the precise geometry, i.e., the multilayer reconstruction and relaxation of the surface at low temperature have only been addressed recently. At temperatures below about 230 K, the low-energy electron diffraction (LEED) pattern indicates a phase transition to a $c(2 \times 2)$ structure.^{2,3} DK (Ref. 1) proposed that the surface atoms displaced alternately along the $\langle 110 \rangle$ directions, forming zigzag chains perpendicular to the atomic displacements (Fig. 1). This structure corresponds to an M_5 -point phonon of the ideal surface. Although there is no reason for the reconstruction to be confined to the surface layer only, experimental and theoretical limitations restricted the analyses of experimental data in the following years⁴ to consideration of only lateral shifts of the surface-layer atoms and the contractions of the first-interlayer distance. It was only recently that Altman *et al.*⁵ carried out measurements of multilayer reconstruction and relaxation, using the technique of x-ray diffraction. They found that a lateral displacement of the second-layer atoms of about 0.05 Å, or about 20% of that of the first-layer atoms, must be assumed to provide a good fit to the x-ray intensity variation. On the theoretical side, the only existing first-principles investigation of the multilayer reconstruction was carried out by Fu and Freeman,⁶ using a five-layer slab. In this study, the reconstruction in the surface and subsurface layers and the relaxation of the first layer were allowed for, leaving open the question⁵ whether the deeper layers show any significant reconstruction. The only other theoretical study⁷ is a model calculation

within tight-binding framework.

The nature of the high-temperature phase and of the phase transition is a more complex and still unsettled issue. The early LEED experiment appeared to indicate that the high-temperature phase is unreconstructed.³ But a high-energy ion-scattering experiment in 1979 by Stensgaard *et al.*⁸ indicated that the surface atoms are already displaced at room temperature. The idea of a disordered high-temperature phase was, however, not immediately accepted and results of various experiments were still interpreted in favor of the ideal (unreconstructed) surface.⁴ Relevant theoretical studies on this issue appeared in 1985. Fu *et al.*⁹ calculated the energy difference between the relaxed ideal surface and the reconstructed surface. Based on the result (about 10

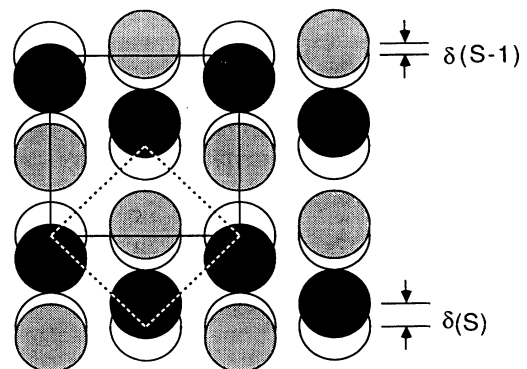


FIG. 1. Top view of the reconstructed W(001) surface. Atoms in the surface and subsurface layers are denoted by solid and shaded circles, respectively. The open circles represent the ideal positions of the atoms. The primitive cells of the reconstructed and ideal surfaces are outlined by solid and dashed lines, respectively.

meV), the authors concluded that it was consistent with a phase transition from the ideal surface to the DK reconstruction at the observed temperature. Their result is, however, very different from the subsequent studies by Singh and co-workers.^{10,11} The latter found the energy difference between the two structures to be about 90 meV (1044 K in temperature units). Since the actual transition occurs at about 250 K, Singh and co-workers^{10,11} concluded that the high-temperature phase is not likely the ideal surface, in support of the experimental result of Stensgaard *et al.*⁸ Because of the complexity of the problem, the subsurface and the deeper atoms were confined to their bulk positions in these initial studies. However, since the displacement of the atoms beneath the surface layer may effect the energetics, it is important to include consistently these effects.

In this paper, we present results of first-principles calculations on the multilayer reconstruction and relaxation of the W(001) surface. First-principles total-energy and force calculations are carried out using the all-electron linearized augmented-plane-wave (LAPW) method¹² within the local-density approximation (LDA).¹³ A thicker slab (of seven atomic layers) in the supercell geometry was used to simulate the surface and all atoms were free to relax within the symmetry constraints. To investigate the above-mentioned issues, we determined the equilibrium geometries for the DK reconstructed surface and the relaxed but unreconstructed surface. The task of finding the equilibrium geometries is greatly facilitated by the recently achieved capability¹⁴ to accurately calculate atomic forces within the LAPW method. The energy difference between the two structures was also obtained and results are compared with experiment and previous calculations. In the second part of the paper, we will present and discuss the electronic band structure of the equilibrium reconstructed surface.

As mentioned, the W(001) surface is modeled by a seven-layer slab. The slab is repeated normal to the surface with vacuum regions equivalent to five atomic layers of W separating the slabs. The in-plane lattice constant is taken to have the experimental value $a = 3.16 \text{ \AA}$. The Wigner interpolation formula¹⁵ is used for the exchange-correlation potential, which gives an excellent equilibrium lattice constant (to within 0.2% of the experimental value) for bulk W.¹⁶ The muffin-tin radii are chosen to be $R = 2.3 \text{ a.u.}$ The kinetic-energy cutoff for the basis functions is given by $k_{\text{max}} = 8.5/R$, which leads to a set of about 2200 LAPW's. To test the convergence of the calculation with respect to this kinetic-energy cutoff, we repeated the calculation using $k_{\text{max}} = 9/R$. The resulting atomic forces are found to be different by only 0.1 mRy/ a_B for the same atomic geometry, indicating a high level of convergence. The potentials of angular momentum of up to $l = 4$ are included in the muffin-tin spheres. Test calculations including potentials up to $l = 8$ give forces that differ by 1 mRy/ a_B . The core states are treated fully relativistically and the valence states semirelativistically (i.e., the spin-orbit interaction is neglected). The 5p semicore states are treated variationally in a second energy window. Considering the highly asymmetric potential near the surface, this treatment of the

relatively extended 5p semicore state is better than treating it as a core state using the spherical-potential approximation. The accuracy of the two-window approach was confirmed by performing some parallel calculations using a modified LAPW method¹⁷ in which the orthogonality of the valence states with the semicore states is guaranteed. The Brillouin-zone (BZ) sampling consists of one \mathbf{k} point in the semicore window and four special \mathbf{k} points in the valence-state window. According to previous work,^{10,11} increasing the number of \mathbf{k} points from 4 to 16 does not significantly change the energy difference between two geometries. A temperature broadening of 1 mRy is used to reduce the finite- \mathbf{k} -point effects.

The force calculation using the LAPW method has been tested in frozen-phonon calculations on bulk systems and the calculated forces were shown to be within a few percent of the total energy results.¹⁴ We have also performed tests on a phonon frequency in bulk bcc W; the results are similar to those reported earlier.¹⁴ The present surface study, of course, provides a far more stringent test, since the equilibrium positions are not symmetry positions and the components of the force must therefore cancel correctly to arrive at the correct equilibrium geometry. We began our calculation with the atoms near the reconstruction geometry (without relaxation) as determined by a recent x-ray-diffraction experiment.⁵ The forces are calculated after charge-density self-consistency was nearly attained. Initially, the forces on the surface atoms were of the order of 20 mRy/ a_B laterally and 50 mRy/ a_B vertically. The values indicate that the equilibrium positions are a few percent of the lattice constant away from this configuration. The atoms were then moved according to the forces and iterations to self-consistency were again performed. The total energy were found to decrease with the magnitude expected from the forces. This process was repeated several times until the forces were reduced to less than 3 mRy/ a_B in all directions. The change in the total energy between the last two configurations is approximately 0.1 mRy per surface atom. As the forces and the changes in the energy were sufficiently small, we took our last geometry as our equilibrium geometry.

The reconstruction and relaxation parameters of the equilibrium geometry are given in Table I, together with the results of the previous theoretical^{6,7} and experimental work.⁵ Uncertainties associated with our values are estimated from the residual forces and are also given in Table I. There is an appreciable scatter in the values for the lateral shift of the surface atoms. Our value of $\delta(S) = 0.268 \text{ \AA}$ is near the upper limit of the x-ray-diffraction experimental value, while that of Fu and Freeman⁶ (0.22 \AA) is at the lower end of the experimental error range. This discrepancy already was present in earlier work^{6,9-11} that considered the reconstruction of the surface layer only. (The origin of the discrepancy is still unresolved and is discussed further below.) The result of Legrand *et al.* appears to be in better agreement with experiment. One must note, however, that the error bar of the experimental result is large enough to allow all of the theoretical results. Results of previous LEED experiments, which favor the smaller lateral shift, are under-

TABLE I. Comparison of the theoretical and experimental lateral displacements of the surface and subsurface layer atoms and percentage change in the first- and second-interlayer spacings of the low-temperature W(001) from the bulk-truncated geometry.

	Present work	Fu and Freeman ^a	Legrand <i>et al.</i> ^b	Experiment ^c
$\delta(S)(\text{\AA})$	0.268 ± 0.005	0.22	0.25, 0.18	0.24 ± 0.025
$\delta(S-1)(\text{\AA})$	0.048 ± 0.002	0.05	0.05	0.046 ± 0.016
$\delta(S-2)(\text{\AA})$	0.015 ± 0.002			
$\delta(S-3)(\text{\AA})$	0.006 ± 0.002			
$\Delta_{12}(\%)$	-6 ± 0.5	-4	-2.1, -1.5	-4 ± 10
$\Delta_{23}(\%)$	0.5 ± 0.5		-0.9, -0.6, -0.3	

^aReference 6.

^bReference 7.

^cReference 5.

mined by the inherent assumption that the reconstruction is confined to the first layer and thus the comparison may not be very meaningful. The theoretical values for the lateral shift of subsurface atoms are in surprisingly good agreement with each other and with experiment. We further find the lateral shift of the third and fourth (the center layer in our calculation) to be 0.015 and 0.006 Å, respectively, with an uncertainty of 0.002 Å. The displacement of the center-layer atoms may be larger than what it should be as a result of the slab geometry. On the other hand, its small value suggests that finite-size effects do not affect the surface and subsurface layers significantly. We note that the results show an exponential decay of the lateral displacement with the distance from the surface, with the decay length being on the order of the interlayer distance.

A contraction in the spacing between the surface and subsurface atomic layers, d_{12} , is predicted by all theoretical work. The results range from a change of 2% of Legrand *et al.*⁷ to our 6%. The recent x-ray-diffraction experiment⁵ cannot resolve these differences because the x-ray intensity variation is insensitive to the vertical displacements of surface atoms. An early detailed analysis of the low-temperature LEED spectra¹⁸ favors a larger value (6%). However, the shift of the subsurface atoms was not considered in the analyses. We also predict an expansion in the second interlayer spacing (d_{23}). The magnitude of the expansion is, however, much smaller than that of the first interlayer contraction. By contrast, Legrand *et al.*⁷ predicted a contracted rather than expanded second interlayer spacing. The contraction-expansion (contraction in the first- and expansion in the second-interlayer spacing) relaxation behavior of metal surfaces has been found for other metallic surfaces.¹⁹ First-principles calculation of the multilayer relaxation of unreconstructed W(001) also predicts an expansion of the second-interlayer spacing (see below). It is then not surprising that the expansion persists after the reconstruction. The change in the spacing between the third and fourth layers is found to be minimal (0.1%). These values are reduced significantly from the corresponding values for the unreconstructed W(001) surface (see below).

In an earlier paper¹¹ in which calculations were per-

formed using the same computer code, but in which the extended $5p$ semicore states were treated as core states, the relaxation of the surface layer was examined but was found to be very small, in contrast with the present prediction of a 6% contraction. Part of the difference arises from the lateral shift of the subsurface atoms in the present work, which tend to reduce the first-interlayer spacing. To understand the remaining differences, we have repeated the calculations by treating the $5p$ states as core states for two geometries: the equilibrium surface geometry as reported above and the unrelaxed surface with exactly the same lateral shifts. It is found that the total-energy difference between the two geometries is small (1 mRy/cell) but favors the unrelaxed geometry. We believe that this result arises from the treatment of $5p$ state as a core state, wherein the spherical-potential approximation is made, and this may not be adequate because the potential is highly asymmetric *normal* to the surface. This is supported by the fact that the lateral components of the calculated forces agree quite well whereas the normal components are significantly different. In the unrelaxed geometry, the vertical component of the force on the surface atoms is smaller when the $5p$ state is treated as a core state than when it is treated variationally in a second energy window. This is consistent, of course, with the previous finding that the surface would undergo small relaxation.

The accuracy of the two-window approach cannot be ascertained *a priori* because the valence states are not exactly orthogonal to the $5p$ semicore states. Thus, a further test was carried out using a modified LAPW method.¹⁷ In this test, the $5s$ and $5p$ semicore states and the valence states were placed in a single energy window thereby ensuring the orthogonality between the valence and the semicore states. Besides the usual LAPW basis functions, additional basis functions that are localized inside the muffin-tin spheres were included. These local basis functions consist of linear combinations of the valence and semicore muffin-tin orbitals for $l \leq 2$ such that the functions and their first radial derivatives vanish on the muffin-tin spheres. The $l=2$ local orbitals were used to reduce any residual errors which may arise due to the linearization of the $5d$ bands. The above determined equilibrium surface and the unrelaxed surface with exact-

ly the same lateral shifts were again studied. The total-energy difference between the two geometries decreased by only 12% from the two-window calculations. To put this into perspective, this will change, for example, the first-interlayer spacing by less than 0.5%. The closeness of the results certainly suggests that the nonorthogonality in the two-window calculations is not significant in the calculated total-energy differences or the atomic forces for W.

The nature of the phase transition (i.e., order-order, order-disordered, etc.) is still somewhat controversial. Originally, the surface was thought to be relaxed but unreconstructed at room temperature (order-order phase transition). The high-energy ion-scattering experiment of Stensgaard *et al.*⁸ and other recent experiments^{20–23} have cast doubt on this view. Instead, the surface may be disordered at room temperature. Theoretically, a quantity relevant to this question is the energy difference (ΔE) between the ideal (relaxed) surface and the reconstructed surface. This quantity has now been calculated a number of times.^{6,9–11} The results, as given in Table II, are scattered over a wide range. The first calculation carried out by Fu *et al.*⁹ gave a value of only 10 meV per surface atom, which they conclude is consistent with an order-order transition (i.e., ideal high-temperature surface). The subsequent calculation by Singh *et al.*,¹⁰ on the other hand, yielded a large value of 106 meV per surface atom (1230 K in temperature units). The authors concluded that the high-temperature phase was not the ideal structure because the transition in consideration takes place at about 250 K. The discrepancy between the calculations of Fu and Freeman⁶ and the present work is still large (see below). (Different approaches were used in the calculations carried out by the two groups. The exact origin of the discrepancy is unknown, however.)

Due to the complexity of the problem, the results just mentioned were obtained by considering the surface-layer reconstruction only. The effect of the underlayers have only partially been addressed recently. Fu and Freeman⁶ calculated ΔE by including the atomic shift of the subsurface atoms and obtained a much larger $\Delta E = 60$ meV per surface atom. The result underscores the importance of the contribution of the underlayers. We have therefore recalculated ΔE with the atomic shift in deeper layers consistently taken into account. To this end, the multilayer relaxation of the ideal surface was investigated using the same supercell and the same parameters. We

TABLE II. Total-energy difference (in meV per surface atom) between the relaxed unreconstructed surface and the reconstructed surface as obtained by various calculations.

Fu <i>et al.</i> ^a	Fu and Freeman ^b	Singh <i>et al.</i> ^c	Singh and Krakauer ^d	Present work
10	30,60 ^e	106	90	110

^aReference 9.

^bReference 6.

^cReference 10.

^dReference 11.

^eThe shift of second-layer atoms is included.

found that d_{12} (the first-interlayer distance) is reduced by 10%, d_{23} is increased by 5%, and d_{34} is increased by about 1%. The relaxation energy, i.e., the energy decrease as a result of the relaxation is 114 meV per surface atom. These values are much larger than those found earlier by Fu *et al.*,²⁴ where the $5p$ states were treated as core states. The energy difference between the fully relaxed ideal surface and the DK reconstructed surface is 8.0 mRy (~ 110 meV) per surface atom, which is comparable to the value obtained by Singh and co-workers.^{10,11} Our calculation affirms the previous conclusion^{10,11} that the high-temperature phase is not the unreconstructed surface.

We now turn to the electronic structure of the equilibrium low-temperature W(001) surface. So far, the theoretical band structure from first-principles study has only been published for the unreconstructed surface.^{25,26} One notable feature of the band structure of the unreconstructed surface is the presence of surface states (SS) crossing the Fermi level not far from the midpoint between Γ and M . The SS thus nest with their inversion images, with the nesting vector being close to the observed wave vector associated with the reconstruction. This nesting of the SS was previously²⁷ used to support the charge-density-wave (CDW) mechanism²⁸ for the phase transition. While the CDW mechanism may not explain the reconstruction, the presence of the Σ_2 SS is important for this reconstruction (see below). The theoretical band structures have been compared with the room-temperature experimental result^{29–31} and found to

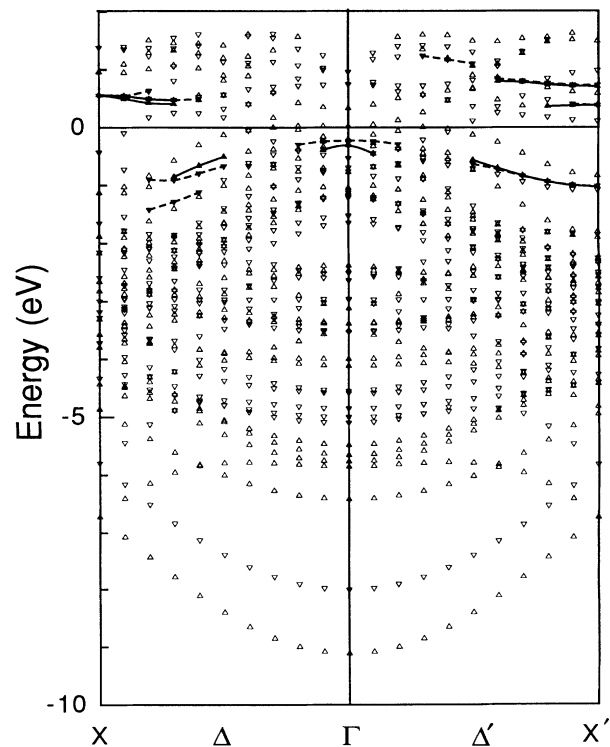


FIG. 2. Electronic band dispersions for the equilibrium reconstructed W(001) surface along the high-symmetry directions.

be in reasonable agreement. However, there remain discrepancies. For example, the experiments of Holmes and Gustafsson³¹ and of Smith *et al.*³² all show that the surface states along Σ cross the Fermi level closer to M than the theories predict. But according to yet another experiment,³³ the Σ_2 SS does not cross the Fermi level at all. The confusion among experiments and the discrepancy between theory and experiments are no doubt in part a result of the disorder in the room-temperature surface. If the DK model for the low-temperature phase is correct, a better comparison can be made between the theoretical and experimental band structure for the low-temperature phase. In the following, we report the band structure for our theoretically determined low-temperature equilibrium surface.

The dispersion of the Kohn-Sham eigenvalues of the above-determined W(001) equilibrium reconstructed surface is shown in Fig. 2. The symmetry lines Δ and Δ' , which correspond to the Σ line of the surface Brillouin zone (SBZ) for the ideal surface, are parallel and normal to the zigzag chains, respectively. Since the seven-layer film possess reflection symmetry in the xy plane, the states are either even or odd under z reflection. The even and odd symmetry states are represented by triangles and inverted triangles (point downward), respectively. We indicate the states that have 65% or more of their charge density in the two surface layers by the solid (dashed) lines for even (odd) symmetry states under z reflection. These states are well localized on the surface layers and are thus surface states or resonances (we will call them SR except where an explicit identification is made). We first look at the SR around the zone center right below the Fermi energy. At the Γ point, the odd-symmetry state (with respect to z reflection) has $\approx 90\%$ of the charge in the surface layers while the even-symmetry state has $\approx 75\%$. Away from the zone center, the state assumes the Δ_1 and Δ'_1 symmetry (i.e., even with respect to the reflection in mirror planes along $\langle 11 \rangle$). The states disperse slowly downward (the odd-symmetry state of the pair appears to have little dispersion) and become delocalized rapidly. The charge density of the odd-symmetry state of the pair is shown in Fig. 3. The density distribution is very similar to that of the so-called Swanson-hump

state³⁴ on the bulk-truncated surface (compare Fig. 8 of Ref. 25), except for the distortion arising from the reconstruction of the surface. It is interesting that this state survives the reconstruction given its sensitivity²⁵ to the self-consistency in the surface potential. The average binding energy of the state is about 0.3 eV, which is close to the room-temperature experimental value²⁹ and the theoretical result for the bulk-truncated surface.²⁶

Another occupied SS appears toward the zone boundary X' (this is the direction of the atomic displacement and the wave vector of the frozen-in phonon, for definiteness in the following discussion, we shall refer to it as $[110]$). The even- and odd-symmetry states with respect to the z reflection are almost degenerate. The state is of the Δ'_2 symmetry, i.e., odd with respect to the $(1\bar{1}0)$ reflection. This is a true SS near X' since it is located in the large energy gap of states of this symmetry. About halfway between Γ and X' it disappears into the region occupied by bulk bands. The state has a binding energy of 1.0 eV and is highly localized on the surface layer at X' . As it moves toward Γ along Δ' it disperses upward and slowly delocalizes. Figure 4 shows the charge density of the state at X' . The state consists primarily of $d_{x^2-y^2}$ and $d_{(x-y)z}$ orbitals. The former forms strong bonds between neighboring atoms within the zigzag chains [Fig. 4(a)].

The above bonding SS at X' is clearly evolved from the Σ_2 SR on the ideal surface. The reconstruction in the $[110]$ direction creates a perturbation which splits the state in two at X' , producing bonding and antibonding states. The antibonding state is located at 0.7 eV above the Fermi energy (second unoccupied SR). Like the bonding state, the antibonding state is a true SS at X' and is very strongly localized on the surface layer. The localization diminishes as one moves away from X' . Between $0.3k_{\Gamma X'}$ and $0.5k_{\Gamma X'}$ one still finds the odd component (under z reflection) of the Δ'_2 symmetry. The connectivity with the state extends from X' is somewhat obscure. The antibonding nature is apparent in the charge-density plot of the state at X' in Fig. 5. Notice that the $d_{(x-y)z}$ orbital here has a larger weight than the $d_{x^2-y^2}$ orbital compared with the bonding state (Fig. 4). (The contrast be-

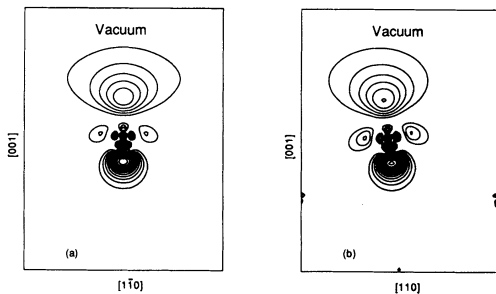


FIG. 3. Contour plot of the charge density of the Swanson-hump state at Γ in two vertical planes both going through a surface atom. Charge density is normalized to one electron per supercell. Contour lines are separated by 0.0015 electrons per supercell.

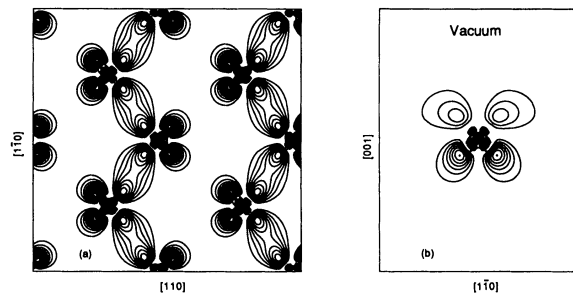


FIG. 4. Charge density (normalized to one electron per supercell) of the bonding X'_2 state in (a) the plane of the surface atoms and (b) a vertical (110) plane going through a surface atom. Contour lines are separated by 0.0015 electrons per supercell.

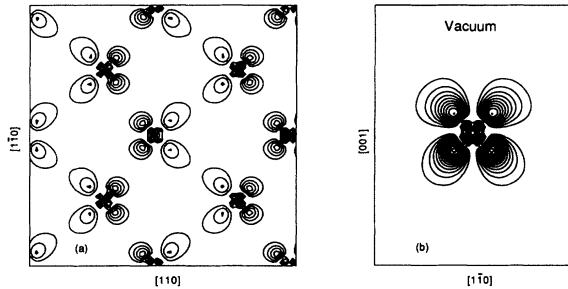


FIG. 5. Charge density of the antibonding X'_2 state. Charge normalization and contour step are as in Fig. 4.

tween the bonding and antibonding states appears to be sharper here than Fig. 3 of Fu and Freeman.⁶) In contrast with the Δ'_2 SS, we do not find any Δ'_1 -symmetry SR near the X' point in the occupied bands. A SR of this symmetry exists at about 0.4 eV above the Fermi level. It is, however, not as localized as the Δ'_2 states (only about 70% of charge is on the surface atoms).

The SR along Δ are changed significantly by the reconstruction as well. Despite the fact that this direction is perpendicular to the $[110]$, no well-defined SR crosses the Fermi level here as in the case of the ideal surface. In general, the SR in this direction are less localized on the surface. A SS of the Δ_2 symmetry [note the (110) reflection is associated with a nonprimitive translation], is visible from 0.5 to $0.8k_{\Gamma X}$ at the binding energy of less than 1 eV. For this state only about 75% of the charge is localized on the surface atoms at its maximum (near $0.7k_{\Gamma X}$). Near the zone boundary X , the state becomes more delocalized (more charge moves to the $S-2$ layer). This is reflected in the large splitting between the even and odd (under z reflection) states. In Fig. 6, we plot the charge density of this state at $0.7k_{\Gamma X}$. It is readily seen that the bonding between the surface atoms is different from the SS at X' and is weaker in the surface layer. A SR of the Δ_1 symmetry lies not far below the Δ_2 state. Only the z -reflection odd state is visibly localized, with nearly 70% of the charge in the surface layer. Finally, two unoccupied SR, one of each symmetry [even and odd under (110) reflection] exist near the X point at about 0.55 eV. These two states are degenerate at X by symmetry.

Very limited experimental results regarding the elec-

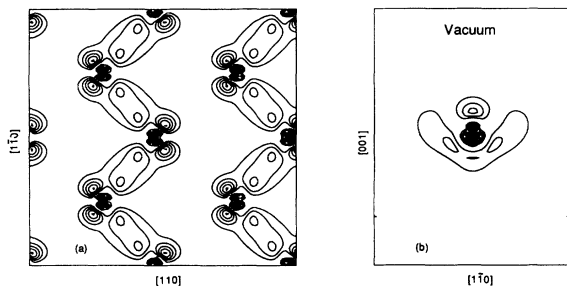


FIG. 6. Charge density of the surface resonance Δ_2 at $0.7k_{X\Gamma}$. Charge normalization and contour step are as in Fig. 4.

tronic structure in the low-temperature phase are available at the present. As far as we know, there has been only one photoemission experiment^{30,33} performed at low temperature and the photoemission spectra were recorded at only a few \mathbf{k} points. According to the results, the SS that crosses the Fermi level at the midpoint of ΓM disappears on cooling the surface from room temperature. On the other hand, at a neighboring \mathbf{k} point along Σ , these states were found to be almost intact. The disappearance of the SS at the midpoint of ΓM was interpreted as due to the splitting of the SS near the Fermi level in the ideal surface and resulting in the reduction in the density of states. However, this does not agree with our calculated band structure which shows a strong bonding state at X' at about -1.0 eV below E_F which should be observable. The features at about 4.5 and 2.5 eV below E_F that exist in the high-temperature phase and also predicted theoretically for the ideal surface^{25,26} were also observed in the low-temperature phase.³³ These states are not found in the present calculations. This is probably because of the limited thickness of the slab used (the -2.5 -eV state was only identified in the 19 layer slab in the work of Mattheiss and Hamann²⁶). More detailed experimental study of the low-temperature electronic structure of the surface will be useful.

We have already discussed the energy difference between the reconstructed and the unreconstructed surface. We now comment on the mechanism of the reconstruction. Early explanations of the reconstruction were often formulated in terms of the CDW mechanism.^{27,28} One criticism of this simple model is well known: Since the SS in the clean surface does not cross E_F at exactly $\frac{1}{2}k_{\Gamma M}$ (Fig. 7, see also Refs. 26 and 31), the CDW mechanism should predict a maximum instability at a different wave vector than the one actually realized. The subsequent model tight-binding calculations by Terakura *et al.*³⁵ sug-

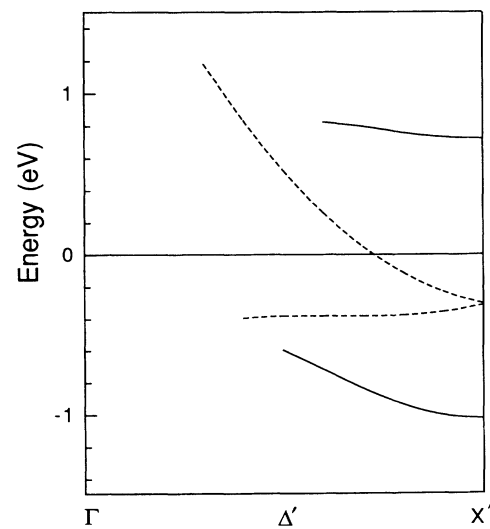


FIG. 7. Comparison of the odd-symmetry surface-state dispersion of the relaxed ideal surface (dashed lines) and of the reconstructed surface (solid lines).

gested that the energy gain in the DK reconstruction was, in large part, due to the bonding of the d orbitals in the SS near E_F . Without including the electron-phonon matrix elements (i.e., bonding effects), the calculated response function did not exhibit a peak for the phonon associated with the reconstruction. Similar results were obtained later by Wang and Weber³⁶ who calculated the phonon spectrum for the unreconstructed surface, but these authors concluded that it was very much the Peierls (i.e., CDW) mechanism that is responsible for the DK reconstruction. From the results of first-principles calculations for different distortions, Singh and co-workers^{10,11} argued for the bonding mechanism. The contribution of the bonding to the instability of the surface is perhaps acknowledged by most authors and is evident in the charge density (see below) and the band structure. In the classical CDW picture, the change in the band structure due to reconstruction is expected to be confined to a small region near X' , at least for small distortions. On the other hand, it is characteristic of bonding that the band structure is affected over a large portion of the BZ. This type of change is seen in Fig. 7 where we compare the band dispersion of the odd-symmetry SS in the reconstructed surface and that in the fully relaxed unreconstructed surface. The same can be observed in the band structure for small atomic displacements (see Fig. 3 of Ref. 36). The essence of the bonding versus CDW argument lies in whether the bonding mechanism is dominant. As mentioned above, many experimental results^{8,20-23} have suggested that the high-temperature phase of the W(001) surface is disordered, which is supported by the calculations by Singh *et al.*^{10,11} and the present work. In this disordered phase, the atoms are presumably displaced from their ideal positions as in the low-temperature phase and are ordered locally. Such a disordered high-temperature phase certainly favors the bonding over the CDW interpretation.

The changes in the electronic structure due to the reconstruction are also reflected in the real-space charge density.¹¹ Similar to unreconstructed semiconductor surfaces, one may use the concept of dangling bonds to describe the "bonding" of the ideal W(001) surface.¹¹ In this dangling bond picture, it is these unsatisfied bonds that cause the reconstruction of the ideal surface. In the reconstructed structure, the dangling bond features are replaced by new ones that may be identified with bonding between the surface atoms.¹¹ From the charge density of the SS, we know that the predominant orbitals are of the $d_{x^2-y^2}$ and $d_{(x-y)x}$ types. By comparing the bonding state at X' (Fig. 5) with the corresponding state of the unreconstructed (relaxed) surface (shown in Fig. 8), it is clear that the bonding state has a greater $d_{x^2-y^2}$ component and a smaller $d_{(x-y)z}$ component than the corresponding state of the unreconstructed surface. This shift in orbital character takes place, of course, because the former has a much greater capacity for bonding neigh-

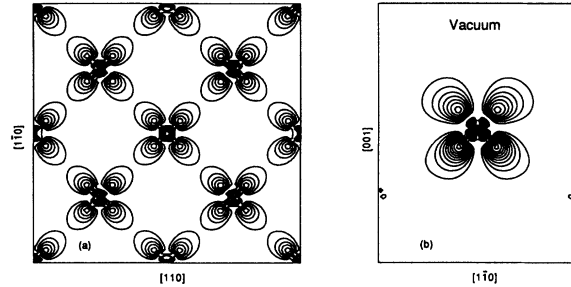


FIG. 8. Charge density of the Σ_2 surface state of the relaxed ideal surface at $\frac{1}{2}k_{\Gamma M}$. Charge normalization and contour step are as in Fig. 4.

boring surface atoms. We may thus further qualify the dangling bond picture by associating these two types of orbitals with the bonding between neighboring surface atoms in the reconstructed surface and the dangling bonds on the unreconstructed surface, respectively.

In summary, we have determined the equilibrium geometry of the low-temperature DK structure of the W(001) utilizing the recently developed capability of force calculations within the full-potential LAPW method. The lateral displacements of the surface and subsurface layers are found to be in good agreement with the recent x-ray experiment of Altman *et al.*⁵ The values for the surface atom displacement and the first-interlayer relaxation are greater than the earlier results of Fu and Freeman.⁶ The differences are not resolved by experiment. The reconstruction and relaxation beyond the subsurface layers are found to be small. We also calculated the energy difference between the fully relaxed ideal surface and the equilibrium reconstructed surface and obtained a value of 110 meV per surface atom, which is close to the previous results of Singh and co-workers.^{10,11} This result affirms the conclusion that the room-temperature phase is not the ideal surface. We have further examined the electronic band structure of our theoretically determined equilibrium surface. No well-defined surface state or resonance crosses the Fermi level. The [110]-reflection odd-symmetry state (Σ_2) of the ideal surface is split by the reconstruction, forming well-defined bonding and antibonding states in the direction of the reconstruction. The so-called Swanson-hump state is also found on the reconstructed surface.

R. Y. and H. K. acknowledge support by National Science Foundation Grant No. DMR-90-22588. D. S. was supported in part by the Office of Naval Research. Computations were carried out at the Cornell National Supercomputer Facility.

- ¹M. K. Debe and D. A. King, *Phys. Rev. Lett.* **39**, 708 (1977).
- ²K. Yonehara and L. D. Schmidt, *Surf. Sci.* **25**, 238 (1971).
- ³T. E. Felter, R. A. Barker, and P. J. Estrup, *Phys. Rev. Lett.* **38**, 1138 (1977).
- ⁴See D. A. King, *Phys. Scr.* T4, 34 (1983), and references therein.
- ⁵M. S. Altman and P. J. Estrup, *Phys. Rev. B* **38**, 5211 (1988).
- ⁶C. L. Fu and A. J. Freeman, *Phys. Rev. B* **37**, 2685 (1988).
- ⁷B. Legrand, G. Treglia, M. C. Desjonqueres, and D. Spanjaard, *J. Phys. C* **19**, 4463 (1986).
- ⁸I. Stensgaard, L. C. Feldman, and P. J. Silverman, *Phys. Rev. Lett.* **42**, 247 (1979).
- ⁹C. L. Fu, A. J. Freeman, and E. Wimmer, and M. Weinert, *Phys. Rev. Lett.* **54**, 2261 (1985).
- ¹⁰D. Singh, S.-H. Wei, and H. Krakauer, *Phys. Rev. Lett.* **57**, 3292 (1986).
- ¹¹D. Singh and H. Krakauer, *Phys. Rev. B* **37**, 3999 (1988).
- ¹²O. K. Andersen, *Phys. Rev. B* **12**, 3060 (1975); D. D. Koelling and G. O. Arbman, *J. Phys. F* **5**, 2041 (1975).
- ¹³D. R. Hamann, *Phys. Rev. Lett.* **42**, 662 (1979); E. Wimmer, H. Krakauer, M. Weinert, and A. J. Freeman, *Phys. Rev. B* **24**, 864 (1981); S.-H. Wei and H. Krakauer, *Phys. Rev. Lett.* **55**, 1200 (1985).
- ¹⁴R. Yu, D. Singh, and H. Krakauer, *Phys. Rev. B* **43**, 6411 (1991).
- ¹⁵E. Wigner, *Phys. Rev.* **46**, 1002 (1934).
- ¹⁶S.-H. Wei, H. Krakauer, and M. Weinert, *Phys. Rev. B* **32**, 7792 (1985).
- ¹⁷D. Singh, *Phys. Rev. B* **43**, 6388 (1991).
- ¹⁸J. A. Walker, M. K. Debe, and D. A. King, *Surf. Sci.* **104**, 405 (1981).
- ¹⁹See, e.g., K. M. Ho and K. P. Bohnen, *Phys. Rev. B* **32**, 3446 (1985).
- ²⁰J. P. Wood and J. L. Erskine, *J. Vac. Sci. Technol. A* **4**, 1414 (1986).
- ²¹I. Stensgaard, K. G. Purcell, and D. A. King, *Phys. Rev. B* **39**, 897 (1989).
- ²²I. K. Robinson, A. A. MacDowell, M. S. Altman, P. J. Estrup, K. Evans-Lutterodt, J. D. Brock, and R. J. Birgeneau, *Phys. Rev. Lett.* **62**, 1294 (1989).
- ²³J. Jupille, K. G. Purcell, and D. A. King, *Phys. Rev. B* **39**, 6871 (1989), and references therein; K. G. Purcell, G. P. Derby, and D. A. King, *J. Phys.: Condens. Matter* **1**, 1373 (1989).
- ²⁴C. L. Fu, S. Ohnishi, E. Wimmer, and A. J. Freeman, *Phys. Rev. Lett.* **53**, 675 (1984).
- ²⁵M. Posternak, H. Krakauer, A. J. Freeman, and D. D. Koelling, *Phys. Rev. B* **21**, 5601 (1980).
- ²⁶L. F. Mattheiss and D. R. Hamann, *Phys. Rev. B* **29**, 5372 (1984).
- ²⁷H. Krakauer, M. Posternak, and A. J. Freeman, *Phys. Rev. Lett.* **43**, 1885 (1979).
- ²⁸E. Tosatti, *Solid State Commun.* **25**, 637 (1978).
- ²⁹S.-L. Weng, E. W. Plummer, and T. Gustaffson, *Phys. Rev. B* **18**, 1718 (1978), and references therein.
- ³⁰J. C. Campuzano, D. A. King, C. Somerton, and J. E. Inglesfield, *Phys. Rev. Lett.* **45**, 1649 (1980).
- ³¹M. I. Holmes and T. Gustaffson, *Phys. Rev. Lett.* **47**, 443 (1981).
- ³²K. E. Smith, G. S. Elliott, and S. D. Kevan, *Phys. Rev. B* **42**, 5385 (1990).
- ³³J. C. Campuzano, J. E. Inglesfield, D. A. King, and C. Somerton, *J. Phys. C* **14**, 3099 (1981).
- ³⁴L. W. Swanson and L. C. Crouser, *Phys. Rev. Lett.* **16**, 389 (1966).
- ³⁵K. Terakura, I. Terakura, and Y. Teraoka, *Surf. Sci.* **86**, 535 (1979); I. Terakura, K. Terakura, and N. Hamada, *ibid.* **103**, 103 (1981).
- ³⁶X. W. Wang and W. Weber, *Phys. Rev. Lett.* **56**, 2295 (1986).

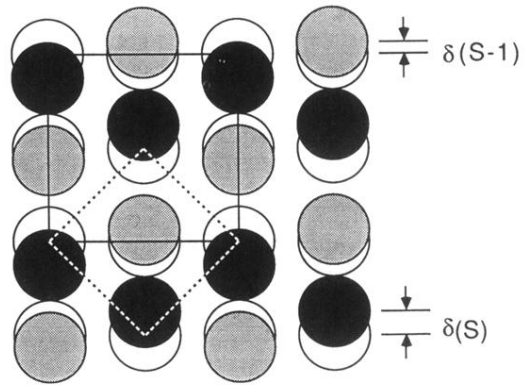


FIG. 1. Top view of the reconstructed W(001) surface. Atoms in the surface and subsurface layers are denoted by solid and shaded circles, respectively. The open circles represent the ideal positions of the atoms. The primitive cells of the reconstructed and ideal surfaces are outlined by solid and dashed lines, respectively.